


Cite this: *RSC Adv.*, 2020, 10, 41202

# Microwave assisted synthesis of negative-charge carbon dots with potential antibacterial activity against multi-drug resistant bacteria

Jung-Chang Kung,<sup>†abc</sup> I-Ting Tseng,<sup>†d</sup> Chi-Sheng Chien,<sup>ef</sup> Sheng-Hui Lin,<sup>eg</sup> Chun-Chi Wang<sup>†\*hi</sup> and Chi-Jen Shih<sup>†\*cdj</sup>

In this research, negative-charge carbon dots (CDs) were synthesized in one-step using a microwave and found to have potential antibacterial ability against multi-drug resistant bacteria. The CDs were synthesized by using citric acid and urea as precursors, and characterized by FT-IR, TEM and fluorescence spectrophotometry. The average size of CDs was about 2.5 nm, and the  $\zeta$  potential was  $-11.06$  mV. In the following antibacterial activity test, time-killing curve experiments and colony-forming assay were carried out to determine the minimum bactericidal concentration (MBC) and minimum inhibitory concentration (MIC) of the CDs against methicillin-resistant *Staphylococcus aureus* (MRSA) and vancomycin-intermediate *Staphylococcus aureus* (VISA). The data showed the MBC of the CDs against MRSA is  $2.5$  mg mL<sup>-1</sup>, and the MIC of the CDs against MRSA is  $0.63$  mg mL<sup>-1</sup>; the MBC of the CDs against VISA is  $1.25$  mg mL<sup>-1</sup>, and the MIC of the CDs against VISA is  $0.63$  mg mL<sup>-1</sup>. The results demonstrated that the negative-charge CDs have potential against multi-drug resistant *Staphylococcus aureus* (*S. aureus*), and may serve as alternatives for therapy in the future.

Received 18th August 2020  
Accepted 15th October 2020

DOI: 10.1039/d0ra07106d

rsc.li/rsc-advances

## Introduction

Multi-drug resistant bacterial infection is an ever-growing threat because of the overuse, inappropriate consumption and wide application of antibiotics. In Taiwan, *S. aureus* which is a Gram-positive bacterium often infecting humans and causing health hazards is commonly found in hospitals.<sup>1</sup> Methicillin is often used in the early stages of infections caused by *S. aureus*, and vancomycin is utilized in the late stages. However, the

abuse of the antibiotics resulted in methicillin-resistant *Staphylococcus aureus* (MRSA) and vancomycin-intermediate *Staphylococcus aureus* (VISA).<sup>2,3</sup> Physical health hazards resulting from multi-drug resistant bacteria have been reported in the literature suggesting that the lethality of multi-drug resistant bacteria will surpass that of cancer by 2050.<sup>4</sup> The requirement to develop new materials against MRSA or VISA is increasing, and the situation is getting worse.

To solve this crisis, the nanotechnology has been developed for anti-bacterial applications. Until now, metal nanoparticles have been found to possess the potential to induce cell death, but the toxicity effect is typically nonspecific.<sup>5-9</sup> Therefore, the relative low toxic carbon nanomaterials were fast developed during the decade. Among the carbon nanomaterials, the carbon dots possess a lot of fantastic properties, such as the high solubility in water, chemically inert property, easy to functionalize, minimal toxicity and good biocompatibility.<sup>10,11</sup> The synthesizing CDs is simple and low-cost that has big economic benefits. Additionally, the fluorescence characteristics and nanoscale distribution make CDs become a research hotspot in various fields.<sup>12</sup> All of those emphasized CDs have a very wide applicability.

Until now, the significant antibacterial effects toward Gram-negative and Gram-positive bacteria have been found in CDs. Dou *et al.* added a bacterial solution and CDs to a culture medium to absorb light at 600 nm. The MIC of the CDs against *S. aureus* and *Escherichia coli* (*E. coli*) was measured.<sup>13</sup> In 2018, Travlou *et al.* discussed the qualitative and antibacterial

<sup>a</sup>School of Dentistry, College of Dental Medicine, Kaohsiung Medical University, Kaohsiung, Taiwan

<sup>b</sup>Department of Dentistry, Division of Family Dentistry, Kaohsiung Medical University Hospital, Kaohsiung, Taiwan

<sup>c</sup>Drug Development and Value Creation Research Center, Kaohsiung Medical University, Kaohsiung, Taiwan

<sup>d</sup>Department of Fragrance and Cosmetic Science, College of Pharmacy, Kaohsiung Medical University, 100 Shi-Chuan 1st Road, Kaohsiung 80708, Taiwan. E-mail: cjshih@gap.kmu.edu.tw; Tel: +886 73121101 ext. 2367

<sup>e</sup>Department of Orthopedics, Chi Mei Medical Center, Tainan, Taiwan

<sup>f</sup>Department of Electrical Engineering, Southern Taiwan University of Science and Technology, Tainan, Taiwan

<sup>g</sup>Department of Leisure and Sports Management, Far East University, Tainan, Taiwan

<sup>h</sup>School of Pharmacy, College of Pharmacy, Kaohsiung Medical University, 100 Shi-Chuan 1st Road, Kaohsiung 80708, Taiwan. E-mail: chunchi0716@cc.kmu.edu.tw

<sup>i</sup>Research Center for Environmental Medicine, Kaohsiung Medical University, Kaohsiung, Taiwan

<sup>j</sup>Department of Medical Research, Kaohsiung Medical University Hospital, Kaohsiung, Taiwan

<sup>†</sup> These authors contributed equally to this work.



capabilities of CDs against *E. coli* and *Bacillus subtilis* after modification with nitrogen and sulphur groups.<sup>14</sup> The method for testing the anti-bacterial capability of CDs in the experiment was the disk diffusion method, which also confirmed the specific antibacterial activity of the CDs. Additionally, in order to know the antibacterial mechanism of CDs, a lot of researches did some measurements to show the mechanism. In 2016, Yang *et al.* proposed that utilization of coating on the quaternary ammonium CDs by electrostatic forces to produce the negative-charge CDs which makes contact with positive-charge bacteria to change the charge balance on the surface of bacteria and further cause the inactivation of bacteria.<sup>15</sup> In 2018, Li *et al.* used TEM, FTIR, XRD, and UV-vis spectroscopy to characterize CDs. Confocal microscopy was utilized to confirm that the CDs entered the fungal cell nuclei to achieve antibacterial effects.<sup>16</sup> This research utilized a variety of strains and showed the antibacterial mechanisms of CDs is to affect the bacterial DNA. In 2019, Yadav *et al.* proved that graphitic carbon nitride quantum dots inhibit *E. coli* and *S. aureus*, and the toxicity is caused by the generation of reactive oxygen species (ROS) in the presence of visible light.<sup>17</sup> The above researches showed the CDs have different mechanisms for antibacterial, and importantly, all of the data demonstrated the different kinds of CDs have the potential against bacterial.

One of the major advantages of CDs is the low cytotoxicity which is much better than metal nanoparticles. In 2014, Wang *et al.* took advantage of the properties of CDs with different functional groups to generate conjugates and form multifunctional imaging probes, and they synthesized CDs by using low-cost and high biocompatible materials, citric acid and urea. Furthermore, cytotoxicity tests was performed with HeLa cells and it was confirmed that the cell survival rate was as high as 96%.<sup>18</sup> In 2017, Liu *et al.* used citric acid and ethylenediamine to synthesize CDs under different temperature conditions and used the mouse osteoblast cell line MC3T3-E1 to test the cytotoxicity of the CDs.<sup>19</sup> The results confirmed that the CDs have a low biotoxicity and good potential for biomedicine. On the basis of the low cytotoxicity of citric acid and urea, and in this study, this concept was followed, and citric acid and urea were used as precursors to synthesize CDs.

Although previous studies have found that CDs lead to a better antibacterial effect on more common strains, such as *Escherichia coli*, *Staphylococcus aureus*, to the best of our knowledge, an evaluation of the antibacterial activity of CDs against MRSA has been rarely reported in the literature. Importantly, the MRSA (ATCC® 33592™) and VISA (ATCC® 700699™) used in this study are common strains of clinical hip joint infection. Therefore, in this study, the microwave assisted synthesis of negative-charge carbon dots from citric acid and urea was applied for against multi-drug resistant bacteria, including MRSA and VISA. The relevance of the dosage, and time to the antibacterial activity and antibacterial dynamics were discussed by estimating the minimal inhibitory concentration (MIC) of the CDs against MRSA and VISA. The negative-charge CDs was hoped to be served as an alternative therapy for infections caused by MRSA and VISA in the future.

## Materials and methods

### The synthesis of CDs

Urea and citric acid (Merck, Darmstadt, Germany) were used as the precursors for the synthesis of CDs by a microwave. First, 3 g urea and 10.5 g citric acid were added to a 50 mL volumetric flask, and then, 18.2 MΩ cm (Milli-Q, Millipore) ultrapure water was added to the volume. After a homogeneous mixture of urea and citric acid, the solution was transferred to Teflon tubes, which were put in a microwave system (CEM, Mars 6). The synthesis condition of the microwave was set at 800 watts, heated at 200 °C for 15 minutes. After the reaction of the microwave, the Teflon tubes were kept in machine for 30 min for cooling down, and then, the solution was filtered through a 0.22 μm pore size filter. Subsequently, the CDs solution was dialyzed with a dialysis membrane (3500 dalton MW) for 4 h, and all the processes should be performed away from light. Finally, the dialysis CDs solution was stored in the 4 °C refrigerator before use.

### Determination of physical properties of CDs

To realize the characterizations of the CDs, the morphology of the CDs was analyzed by transmission electron microscopy (TEM), the particle size and zeta potential of the CDs were characterized by the dynamic laser scattering (DLS), and the bonding and spectral properties of the CDs were measured by UV/vis spectrophotometry, fluorescence spectrophotometry and Fourier transform infrared spectroscopy.

### The cultures of MRSA and VISA

The MRSA and VISA strains were all obtained from the Bio-resource Collection and Research Center (BCRC), and the microbial freeze-dried tubes were inoculated in the specified medium after they were opened, according to the BCRC instructions. The freezing containers were kept and set in a refrigerator at −80 °C. After the solution was completely frozen, it was moved to a storage box for microtubes. The mode used to active the bacteria is performed according to the strain's activity; the frozen medium was removed and placed into a broth. In accordance with the culture condition, the culture was cultivated for 24 h. By the streak-plate method, the agar was inoculated for 24 h and then used as a spare (Table 1).

### Bacterial incubation and antibacterial activity

In this research, MRSA (ATCC 33592) and VISA (ATCC 700699) were selected for the antibacterial activity tests of the CDs.

**Time-killing curves.** The time-killing curves were plotted to determine the antibacterial ability of the CDs against the MRSA

Table 1 Culture conditions of MRSA and VISA

Scientific name	MRSA and VISA
Culture conditions	32.5 ± 2.5 °C
Culture time	24 h
Medium	Tryptic soy agar



and VISA strains. The strains were inoculated in tryptic soy agar by a streak-plate method and cultivated at  $32.5 \pm 2.5^\circ\text{C}$  for 24 h. A single colony was selected and diluted with broth to a concentration of  $10^8$  (turbidity = 0.5). The colony solution was subsequently diluted by sterilized water and broth in a 96 well plate. The bacterial growth is recorded by the OD<sub>600</sub> value.

**Colony forming assay.** A colony forming assay can evaluate the *in vitro* cell survival ratio based on the ability of a single bacterium to grow into a colony. The bacterial growth cycle enters a declining period after 24 h, so this assay method takes 24 h to determine whether the test substance has an effect on the growth ability of each bacterium in the population.

## Result and discussion

### Characterization of the CDs

The synthesis of CDs was carried out by using citric acid and urea dissolved in Milli-Q water, and then heated in the microwave for 15 minutes ( $200^\circ\text{C}$ ) to yield the CDs. The CDs were characterized for checking particle size, charge, topography and functional groups. The TEM image of the CDs (Fig. 1) showed a uniform distribution and the spherical shape with particle sizes in the range of 1.0–5.5 nm. The average diameter of CDs was about 2.5 nm by using DLS (insertion in Fig. 1), and that is matched to the particle size distribution curve from the TEM data. In the  $\zeta$  potential test, the average potential is  $-11.06$  mV. The negative charge was confirmed and supported that the charge was produced from the carboxylic acid groups of the citric acid.

In previous research, the CDs, including carbon quantum dots (CQDs;  $\text{sp}^2/\text{sp}^3$  carbon) and graphene quantum dots (GQDs;  $\text{sp}^2$  carbon), can be functionalized with different molecules or other functional groups for labelling, sensing, tissue imaging, and antibacterial applications.<sup>20</sup> Hence, the determination of the functional groups of the CDs is very important for the following applications. In this research, the functional groups of the negative-charge CDs were measured by using the FT-IR instrument and the data was as shown in Fig. 2. The CDs

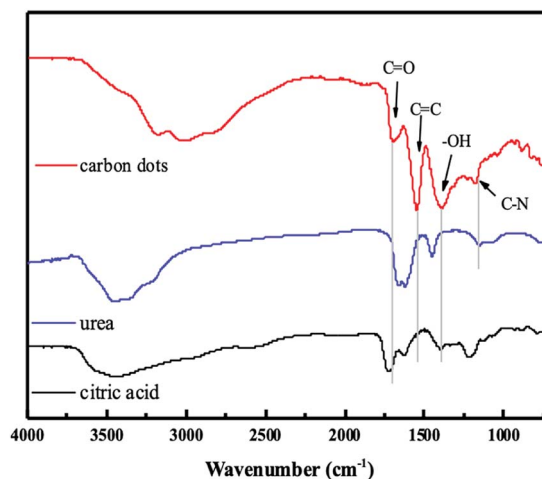


Fig. 2 FT-IR spectra of CDs, urea and citric acid.

possessed several characteristic peaks that were almost similar with those of urea and citric acid. The peak at  $1525\text{ cm}^{-1}$  was attributed from the stretching modes of  $\text{C}=\text{C}$ , which was produced from the polymerization of urea and citric acid and confirmed the successful synthesis of CDs. Additionally, the strong absorption peaks at  $1700\text{ cm}^{-1}$ ,  $1369\text{ cm}^{-1}$ , and  $1164\text{ cm}^{-1}$  are attributed to the stretching modes of  $\text{C}=\text{O}$ ,  $\text{O}-\text{H}$ , and  $\text{C}-\text{N}$ , respectively. These functional groups are also found in the citric acid or urea. As stated above, it can be proved that CDs are successfully synthesized from urea and citric acid.

### Optical properties of the CDs

The CDs usually have apparent optical absorption in the UV-visible region.<sup>21</sup> Most of the CDs, no matter how they are synthesized, possess an absorption band around 260–323 nm. In this study, two major absorption peaks are observed at 240 nm and 332 nm from the negative-charge CDs. The data was as shown in UV-vis spectrum (Fig. 3A). The absorption at 240 nm is ascribed to the  $\pi \rightarrow \pi^*$  electron transition of the  $\text{C}=\text{C}$  band. The strong absorption at 332 nm is attributed to the  $n \rightarrow \pi^*$  transition of the  $\text{C}=\text{O}$  band.

The size-dependent optical absorption or photoluminescence is the classic sign of quantum confinement, which is one of the most exciting features of CDs. Since the results of studies on optical properties of CDs are diverse and controversial, further clarification is required about exact mechanisms of photoluminescence of the CDs.<sup>21–23</sup> The clear reliance of the emission wavelength and intensity on  $\lambda_{\text{ex}}$  is one the fascinating features of the photoluminescence of CDs. Therefore, in this study, various excitation wavelengths were applied to obtain the photoluminescence spectra of the CDs. The photoluminescence spectra was as shown in Fig. 3B. As the excitation wavelengths increase, the maximum photoluminescence wavelengths would also increase. That was the classic photoluminescence property of the CDs and supported that as different energy levels associated with different surface states formed by different functional groups are responsible for

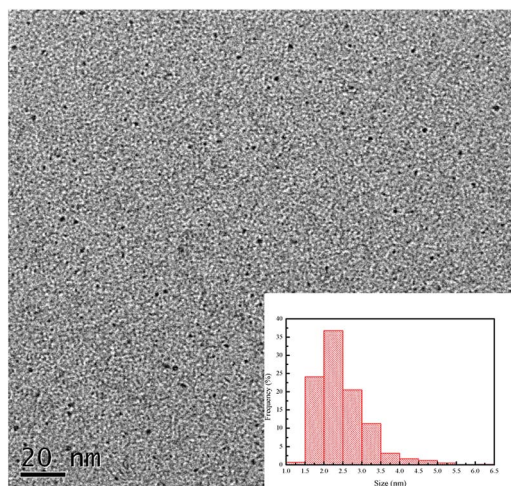


Fig. 1 TEM image and size distribution (inset) of CDs.





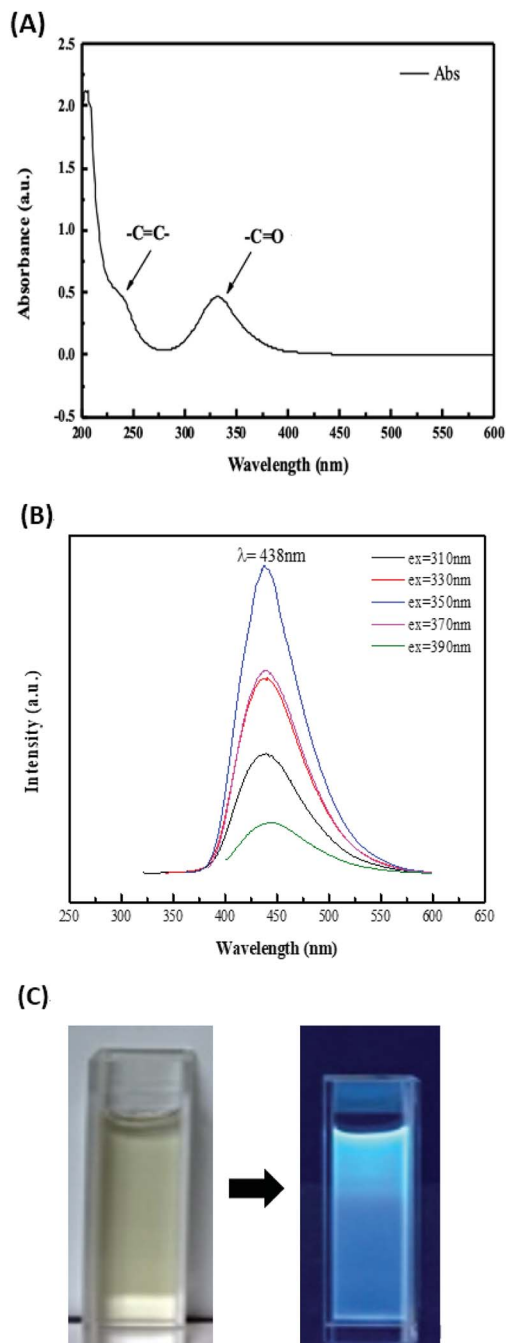


Fig. 3 (A) UV-vis absorption spectrum of CDs. (B) Fluorescence emission spectra of CDs under varied excitation wavelengths. (C) Photographs of CDs under daylight (left) and a UV lamp (365 nm, right).

the excitation-dependent-emission phenomenon, the observed excitation-independent emission over 320–400 nm indicates a relatively uniform and well-passivated CD surface.<sup>24,25</sup> When the excitation wavelength was set at 350 nm, the highest intensity of the photoluminescence of this CDs could be obtained and the maximum photoluminescence wavelength are found at 438 nm. The photographs (Fig. 3C) of the dilute CDs solution is light yellow under daylight and blue under a 365 nm UV lamp. This reveals that the CDs exhibit a blue

photoluminescence response. That was supported the C=O and N-H bonds on the surface of the CDs would result in the blue photoluminescence. That matched the data found in previous research.<sup>26</sup>

### Microbiological assay of the CDs

The CDs have been reported about the ability for inhibiting bacterial growth or killing bacteria through complex mechanisms, including ROS generation, disintegration of cell structure, fragmentation and condensation of genomic DNA, leading to the leakage of the cytoplasm.<sup>27–29</sup> Additionally, the antibacterial ability of CDs can be highly associated with the surface charge and generation of ROS. However, regardless of which mechanism of CDs for antibacterial, increasing the attachment of CDs to the bacterial would increase the efficiency of the antibacterial function of the CDs. Therefore, in this research, the negative-charge CDs was synthesized and confirmed for treatment of the Gram-positive bacterial, MRSA and VISA, to increase the attachment with bacterial through the electrostatic interaction. That was supported the potential of the negative-charge CDs for against Gram-positive bacterial was better than that of the positive or neutral CDs due to the higher interaction, although the positive or neutral CDs also had the anti-bacterial functions. Nevertheless, the Gram-positive bacteria may be killed or inhibited by some antibacterial drugs. Therefore, in this study, the multi-drug resistant bacteria, including MRSA and VISA were chosen as the targets to test the potential of this negative-charge CDs against bacterial.

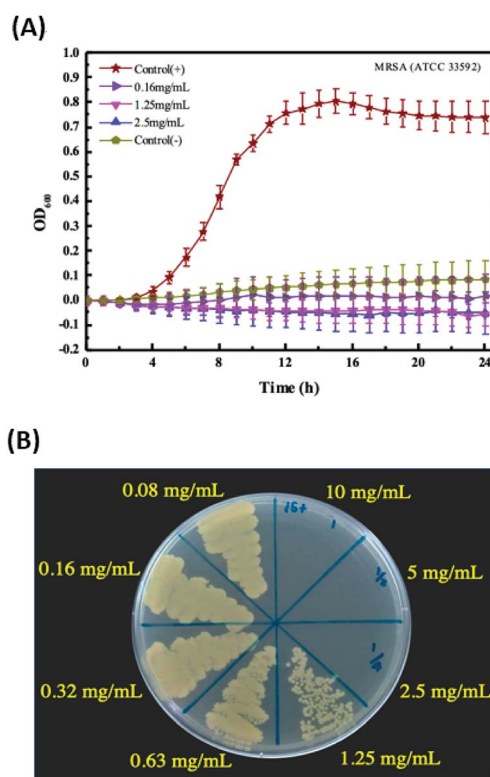


Fig. 4 (A) The time-killing curve result of CDs against MRSA 33592. (B) The colony-forming capacity assay result of CDs against MRSA 33592.

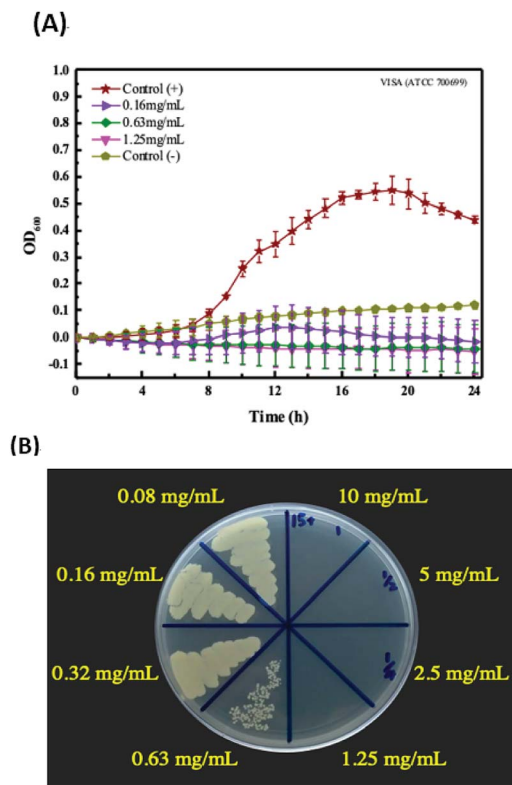


Fig. 5 (A) The time-killing curve result of CDs against VISA 700699. (B) The colony-forming capacity assay result of CDs against VISA 700699.

**CDs against the MRSA.** After calculation of CDs content, the CDs were diluted to  $10 \text{ mg mL}^{-1}$  to facilitate the following experiments. The CDs were diluted with sterilized water, and  $10 \mu\text{L}$  of a  $0.5$  optical density value bacterial solution was added to conduct the antibacterial experiments and prepare the  $24 \text{ h}$  time-killing curves. According to the result of the  $24 \text{ h}$  time-killing curves, at the MRSA bacterial concentration of  $5 \times 10^5 \text{ CFU mL}^{-1}$ , an obvious antibacterial effects was observed with the CDs concentration of  $1.25 \text{ mg mL}^{-1}$  (Fig. 4A). When the CDs concentration was  $0.16 \text{ mg mL}^{-1}$ , MRSA had some growth consequences, and the antibacterial effect is less obvious. In the

colony forming assay (Fig. 4B), it can be observed that there is no colony growth when the CDs concentration is above  $2.5 \text{ mg mL}^{-1}$ . When the CDs concentration is  $1.25 \text{ mg mL}^{-1}$ , there is a discontinuous colony that is the result of the colony forming assay. The time-killing curves of the CDs solutions with concentrations of  $2.5 \text{ mg mL}^{-1}$  and  $1.25 \text{ mg mL}^{-1}$  show the inhibition of the bacteria activity, from which it is deduced that the MBC of the CDs against MRSA is  $2.5 \text{ mg mL}^{-1}$ , and the MIC of the CDs against MRSA is  $0.63 \text{ mg mL}^{-1}$ .

**CDs against the VISA.** The CDs solution with concentrations of  $0.63 \text{ mg mL}^{-1}$  and above greatly inhibit the bacterial activity of VISA with bacterial concentrations of  $5 \times 10^5 \text{ CFU mL}^{-1}$  (Fig. 5A). Compared to the MRSA antibacterial experiment, the curve obtained with the  $0.16 \text{ mg mL}^{-1}$  CDs rises more, suggesting that the antibacterial effect is less obvious. The colony forming assay of VISA indicates that there is no colony growth with a  $1.25 \text{ mg mL}^{-1}$  CDs concentration (Fig. 5B). A discontinuous colony grows with the  $0.63 \text{ mg mL}^{-1}$  CDs concentration. Because the time-killing curves obtained for the CDs concentrations of  $1.25 \text{ mg mL}^{-1}$  and  $0.63 \text{ mg mL}^{-1}$  show the inhibition of the bacteria activity, it is deduced that the MBC of the CDs against VISA is  $1.25 \text{ mg mL}^{-1}$ , and the MIC of the CDs against VISA is  $0.63 \text{ mg mL}^{-1}$ .

### Comparisons of other CDs for antibacterial

In this study, the negative-charge CDs have been demonstrated with the ability against MRSA and VISA. The Table 2 show the comparisons of various CDs for against bacterial. In previous researches, the normal Gram-positive or Gram-negative bacterial, including *E. coli*, *S. aureus* or *B. subtilis* were usually utilized as the samples to test the CDs potential for against bacterial. Bing *et al.* formed candle-soot CDs having a negative charge with zeta potential of  $-19.5 \text{ mV}$  and an average particle size of  $2.93 \text{ nm}$ .<sup>27</sup> The cell activity of *E. coli* after treated with  $0.3 \text{ mg mL}^{-1}$  of the CDs was about  $80\%$ , and the CDs exhibited the bacteriostatic ability toward *E. coli*. However, when compared with previous CDs for against bacterial, this CDs possessed the potential for against multi-drug resistant bacteria, which is better than other CDs. The antibacterial ability against MRSA

Table 2 The comparisons of various CDs for anti-bacterial<sup>a</sup>

	CDs	Size (nm)	ζ-Potential (mV)	Strain	MIC ( $\text{mg mL}^{-1}$ )	MBC ( $\text{mg mL}^{-1}$ )	Remark
Dou <i>et al.</i> <sup>13</sup>	ND	3.5	ND	<i>E. coli</i>	0.64	ND	
				<i>S. aureus</i>	0.32		
Travlou <i>et al.</i> <sup>14</sup>	N-CDs	6.5	$-6.47$	<i>E. coli</i>	0.16	ND	
	S-CDs	5.0	$-47.18$	<i>B. subtilis</i>	0.32		
Yang, <i>et al.</i> <sup>15</sup>	Negative-charge CDs	4.0	$-16.00$	<i>S. aureus</i>	0.008	ND	
Bing <i>et al.</i> <sup>27</sup>	Negative-charge candle-soot CDs	2.93	$-19.50$	<i>E. coli</i>	ND	ND	$0.3 \text{ mg mL}^{-1}$ of C-dots exhibited the bacteriostatic ability toward <i>E. coli</i>
This study	Negative-charge CDs	2.5	$-11.06$	MRSA	0.63	2.5	
				VISA	0.63	1.25	

<sup>a</sup> ND: no detection.



and VISA of the CDs in this study is bacteriostatic and bactericidal. The possible reason is that MRSA and VISA are Gram-positive bacteria, and negative-charge CDs would enhance the direct contact to positively charged bacteria by electrostatic interaction. When CDs interacted with bacteria, the generated ROS became the major factor for inhibiting bacterial growth. The endogenous ROS generation induced by negative charge CDs was higher than that of positive charge CDs due to the attachment of CD to the surface of MRSA and VISA. The ROS generation may be not very clear in this research. However, the CDs inducing the ROS generation have been reported in a lot of researches.<sup>17,30–32</sup> Therefore, in the future work, we need to conduct further experiments to confirm this speculation.

## Conclusions

In this paper, the microwave assisted synthesis of negative-charge CDs was established by using urea and citric acid, and further applied for the antibacterial testing of multi-drug resistant bacteria (MRSA and VRSA) for the first time, without the assistance of metal ions, doping or surface functionalization. The results of the time-killing curves and colony forming assay confirmed that the CDs have an antibacterial activity against MRSA and VISA. The MIC of the CDs against MRSA is 0.63 mg mL<sup>-1</sup>, and the MBC is 2.5 mg mL<sup>-1</sup>. In addition to MRSA, the MIC of the CDs against VISA is 0.63 mg mL<sup>-1</sup>, and the MBC is 1.25 mg mL<sup>-1</sup>. The data demonstrated the CDs had the ability against MRSA and VISA, and is the first application of CDs for against MRSA and VISA.

## Conflicts of interest

There are no conflicts to declare.

## Acknowledgements

The authors acknowledge support of grants from the Research Project of Ministry of Science and Technology, Taiwan (MOST 107-2221-E-037-001-MY3, MOST 108-2314-B-037-019-MY2, MOST 108-2314-B-384-009), the Special Research Project of Kaohsiung Medical University, Taiwan (KMU-TC108A03-7), the Special Research Project of Kaohsiung Medical University Hospital, Taiwan (KMUH 108-8R69), the Research Project of Chi Mei Medical Center and Kaohsiung Medical University Research Foundation, Taiwan (109CM-KMU-005) and the Special Research Project of Chi Mei Medical Center, Taiwan (CMFHR 10888).

## References

- 1 M. Vogel, *et al.*, Infectious disease consultation for Staphylococcus aureus bacteremia—a systematic review and meta-analysis, *J. Infect.*, 2016, 72(1), 19–28.
- 2 M. E. Stryjewski and G. R. Corey, Methicillin-resistant Staphylococcus aureus: an evolving pathogen, *Clin. Infect. Dis.*, 2014, 58(1), 10–19.
- 3 W. A. McGuinness, N. Malachowa and F. R. DeLeo, Focus: infectious diseases: vancomycin resistance in Staphylococcus aureus, *Yale J. Biol. Med.*, 2017, 90(2), 269–281.
- 4 N. McCarthy, *Deaths From Drug-Resistant Infections Set To Skyrocket*, Infographic Newsletter, 2015, <https://www.statista.com/chart/3095/drug-resistant-infections/>.
- 5 J. A. Lemire, J. J. Harrison and R. J. Turner, Antimicrobial activity of metals: mechanisms, molecular targets and applications, *Nat. Rev. Microbiol.*, 2013, 11(6), 371–384.
- 6 J. L. Huang, *et al.*, Strong near-infrared absorbing and biocompatible cus nanoparticles for rapid and efficient photothermal ablation of gram-positive and-negative bacteria, *ACS Appl. Mater. Interfaces*, 2017, 9(42), 36606–36614.
- 7 S. H. Kuo, *et al.*, Antibacterial activity of BSA-capped gold nanoclusters against Methicillin-resistant Staphylococcus aureus (MRSA) and Vancomycin-resistant Staphylococcus aureus (VISA), *J. Nanomater.*, 2019, 4101293, DOI: 10.1155/2019/4101293.
- 8 P. V. AshaRani, *et al.*, Cytotoxicity and genotoxicity of silver nanoparticles in human cells, *ACS Nano*, 2009, 3(2), 279–290.
- 9 M. E. Samberg, S. J. Oldenburg and N. A. Monteiro-Riviere, Evaluation of silver nanoparticle toxicity in skin in vivo and keratinocytes in vitro, *Environ. Health Perspect.*, 2010, 118(3), 407–413.
- 10 P. Miao, *et al.*, Recent advances in carbon nanodots: synthesis, properties and biomedical applications, *Nanoscale*, 2015, 7(5), 1586–1595.
- 11 J. Hou, *et al.*, A novel one-pot route for large-scale preparation of highly photoluminescent carbon quantum dots powders, *Nanoscale*, 2013, 5(20), 9558–9561.
- 12 X. T. Zheng, *et al.*, Glowing graphene quantum dots and carbon dots: properties, syntheses, and biological applications, *Small*, 2015, 11(14), 1620–1636.
- 13 Q. Dou, *et al.*, Multi-functional fluorescent carbon dots with antibacterial and gene delivery properties, *RSC Adv.*, 2015, 5(58), 46817–46822.
- 14 N. A. Travlou, *et al.*, S- and N-doped carbon quantum dots: surface chemistry dependent antibacterial activity, *Carbon*, 2018, 135, 104–111.
- 15 J. Yang, *et al.*, Carbon dot-based platform for simultaneous bacterial distinguishment and antibacterial applications, *ACS Appl. Mater. Interfaces*, 2016, 8(47), 32170–32181.
- 16 H. Li, *et al.*, Degradable carbon dots with broad-spectrum antibacterial activity, *ACS Appl. Mater. Interfaces*, 2018, 10(32), 26936–26946.
- 17 P. Yadav, *et al.*, Metal-free visible light photocatalytic carbon nitride quantum dots as efficient antibacterial agents: an insight study, *Carbon*, 2019, 152(11), 587–597.
- 18 B. Wang, *et al.*, A mitochondria-targeted fluorescent probe based on TPP-conjugated carbon dots for both one- and two-photon fluorescence cell imaging, *RSC Adv.*, 2014, 4(91), 49960–49963.
- 19 J. Liu, *et al.*, One-step hydrothermal synthesis of photoluminescent carbon nanodots with selective



- antibacterial activity against *Porphyromonas gingivalis*, *Nanoscale*, 2017, **9**(21), 7135–7142.
- 20 A. Anand, *et al.*, Graphene oxide and carbon dots as broad-spectrum antimicrobial agents – a minireview, *Nanoscale Horiz.*, 2019, **4**, 117–137.
  - 21 S. N. Baker and G. A. Baker, Luminescent carbon nanodots: emergent nanolights, *Angew. Chem., Int. Ed.*, 2010, **49**, 6726–6744.
  - 22 Q.-L. Zhao, *et al.*, Facile preparation of low cytotoxicity fluorescent carbon nanocrystals by electrooxidation of graphite, *Chem. Commun.*, 2008, **41**, 5116–5118.
  - 23 W. L. Wilson, P. F. Szajowski and L. E. Brus, Quantum confinement in size-selected, surface-oxidized silicon nanocrystals, *Science*, 1993, **262**, 1242–1244.
  - 24 X. Zhai, *et al.*, Highly luminescent carbon nanodots by microwave-assisted pyrolysis, *Chem. Commun.*, 2012, **48**, 7955–7957.
  - 25 L. Tang, *et al.*, Deep ultraviolet photoluminescence of water-soluble self-passivated graphene quantum dots, *ACS Nano*, 2012, **6**, 5102–5110.
  - 26 Y. Fan, *et al.*, Blue- And Green-Emitting Hydrophobic Carbon Dots: Preparation, Optical Transition, and Carbon Dot-Loading, *Nanotechnology*, 2019, **30**(26), 265704, DOI: 10.1088/1361-6528/ab0b14.
  - 27 W. Bing, *et al.*, Programmed Bacteria Death Induced by Carbon Dots with Different Surface Charge, *Small*, 2016, **12**, 4713–4718.
  - 28 H.-J. Jian, *et al.*, Super-Cationic Carbon Quantum Dots Synthesized from Spermidine as an Eye Drop Formulation for Topical Treatment of Bacterial Keratitis, *ACS Nano*, 2017, **11**, 6703–6716.
  - 29 S. G. Harroun, *et al.*, Reborn from the Ashes: Turning Organic Molecules to Antimicrobial Carbon Quantum Dots, *ACS Infect. Dis.*, 2017, **3**, 777–779.
  - 30 F. Nichols, *et al.*, Antibacterial Activity of Nitrogen-Doped Carbon Dots Enhanced by Atomic Dispersion of Copper, *Langmuir*, 2020, **36**(39), 11629–11636.
  - 31 R. Knoblauch and C. D. Geddes, Carbon Nanodots in Photodynamic Antimicrobial Therapy: A Review, *Materials*, 2020, **13**(18), E4004.
  - 32 D.-K. Ji, *et al.*, Controlled functionalization of carbon nanodots for targeted intracellular production of reactive oxygen species, *Nanoscale Horiz.*, 2020, **5**(8), 1240–1249.

